

Vibrational properties of three dimensional Penrose tiling

This article has been downloaded from IOPscience. Please scroll down to see the full text article.

1994 J. Phys.: Condens. Matter 6 953

(<http://iopscience.iop.org/0953-8984/6/5/005>)

View [the table of contents for this issue](#), or go to the [journal homepage](#) for more

Download details:

IP Address: 171.66.16.159

The article was downloaded on 12/05/2010 at 14:41

Please note that [terms and conditions apply](#).

Vibrational properties of three-dimensional Penrose tiling

Decheng Tian†‡, Ying Hu† and Zhengyou Liu†

† Department of Physics, Wuhan University, Wuhan 430072, People's Republic of China

‡ International Centre for Material Physics, Academia Sinica, Shengyang 110015, People's Republic of China

Received 14 December 1992, in final form 13 September 1993

Abstract. We calculated the vibrational densities of states for three-dimensional Penrose tiling. Anomalous behaviour at low frequencies is observed. Two crossover frequencies ω_s and ω_c exist. The first can be attributed to crossover from surface phonon excitations to bulk phonon excitations, while the second is explained as crossover from phonon excitations to fracton-like excitations. The phonons follow the scaling law ω^{d-1} , where d is the Euclidean dimension and equals 3 and 2 for the bulk and the surface phonons, respectively. The fracton-like excitations which have a non-extended character follow the scaling law ω^{d_s-1} where d_s is the fracton-like dimension and is shown to equal 3 for the present case.

1. Introduction

The experimental discovery by Schechtman *et al* [1] of a metallic solid phase of Al-Mn alloy with icosahedral symmetry has considerably revived interest in quasi-crystals. One-dimensional (1D) Fibonacci quasi-lattices, as a 1D version of quasi-crystals, have been studied extensively [2–7]. The spectral structure is shown to be a Cantor-like set, with a peculiar self-similarity and multifractal behaviour in their wavefunctions [7]. Choy [8] and Odagaki and Nguyen [9] have investigated the spectral properties of two-dimensional (2D) Penrose lattices. The vibrational densities of states for various 2D quasi-periodic lattices were calculated by Liu and Tian [10, 11]. Similar work for three-dimensional (3D) quasi-crystals was done by Los and Jansen [12] and Los *et al* [13, 14], as well as by Hafner and Krajci [15, 16].

Non-periodicity and self-similarity are the most remarkable properties of quasi-crystals. For example, the primitive icosahedral lattice is invariant under a scaling by τ^3 ($\tau = \frac{1}{2}(\sqrt{5} + 1)$) [17, 18]. Therefore in the sense of the self-similarity of quasi-crystals we can regard them as fractals within some physical lower and upper cut-offs. In fractal lattices, it is found that there is a special kind of vibrational excitation, a fracton [19], and the low-frequency vibrational density $\rho_G(\omega)$ of states has two scaling regimes, namely the phonon regime and the fracton regime, i.e. one has the following relations:

$$\rho_G(\omega) \sim \begin{cases} \omega^{d-1} & \text{for } \omega < \omega_c \\ \omega^{d_s-1} & \text{for } \omega > \omega_c. \end{cases}$$

ω_c is the crossover frequency from phonon to fracton behaviour of the network and d_s is the spectral (fracton) dimension [19–24]. For quasi-periodic lattices, some work has been done on their fractal features. Kohmoto and Banavar [2] obtained the fractal dimension of the Fibonacci lattice which equals its Euclidean dimension (i.e. one), using the mass–volume relationship. In the calculation of vibrational spectra of 2D quasi-crystals, it is found

that these quasi-crystals have fractal dimensions which are also equal to their Euclidean dimensions and that crossovers from phonon to fracton-like excitations exist in the low-frequency region [10, 11].

The aims of this paper are twofold. Firstly we intend to extend our previous study [10, 11] to a 3D Penrose lattice; we expect fracton-like excitations to exist also in 3D quasi-crystals. Secondly we shall show the character of the vibrational excitations in 3D quasi-crystals.

2. Calculation procedures and structure construction

We utilize the widely used recursion method of Haydock *et al* [25, 26] and Nex [27] which is an efficient technique for obtaining the vibrational spectra of an aperiodic system.

Following the Born model, the potential energy of the lattice is expressed as

$$V = \frac{1}{2}(\alpha - \beta) \sum_{i,j}^{NN} [(\mathbf{u}_i - \mathbf{u}_j) \cdot \mathbf{r}_{ij}]^2 + \frac{1}{2}\beta \sum_{i,j}^{NN} |\mathbf{u}_i - \mathbf{u}_j|^2 \quad (1)$$

where \mathbf{u}_i is the small displacement of the i th site about its equilibrium position \mathbf{r}_i , \mathbf{r}_{ij} is the unit vector from site i to site j , α is the bond-stretching force constant and β is the bond-bending force constant; the summation runs over all the nearest neighbours. The vector nature of the elastic force is included naturally in this equation. When α is chosen to equal β , the system considered becomes isotropic.

The local vibrational density of states [23] can be given as

$$\rho_L(\omega) = -(2\omega/\pi) \text{Im} \langle u_i | 1/(\omega^2 - \mathbf{D}) | u_i \rangle = -(2\omega/\pi) \text{Im} \langle u_i | G | u_i \rangle \quad (2)$$

where $G = 1/(\omega^2 - D)$ is the Green function, \mathbf{D} is the dynamical matrix and $|u_i\rangle$ is the displacement vector of site i . The global density of states following Choy [8] and Peng and Tian [23] takes the form

$$\rho_G(\omega) = -(2\omega/\pi) \text{Im} \overline{\langle 0 | G | 0 \rangle} \quad (3)$$

where $|0\rangle$ is the initial vector whose elements are uncorrelated variables chosen from a Gaussian distribution with mean zero and covariance unity.

There are several methods of constructing Penrose lattices: the projection method [28, 29], the section method [30, 31] and the general dual method [32]. In this paper we shall use the projection method.

The 3D Penrose tiling can be obtained by projecting a six-dimensional (6D) regular lattice onto a 3D plane. The 6D space in which the lattice is embedded can be decomposed into two mutually orthogonal 3D subspaces $V_S = (V_E, V_I)$. The basis in V_S can be chosen as

$$\begin{aligned} a_1 &= b(2d, 0, d, 2d, 0, d) \\ a_2 &= b(2d \cos \phi, 2d \sin \phi, d, 2d \cos(2\phi), 2d \sin(2\phi), d) \\ a_3 &= b(2d \cos(2\phi), 2d \sin(2\phi), d, 2d \cos(4\phi), 2d \sin(4\phi), d) \\ a_4 &= b(2d \cos(3\phi), 2d \sin(3\phi), d, 2d \cos \phi, 2d \sin \phi, d) \\ a_5 &= b(2d \cos(4\phi), 2d \sin(4\phi), d, 2d \cos(3\phi), 2d \sin(3\phi), d) \\ a_6 &= (0, 0, 1, 0, 0, -1) \end{aligned}$$

where $b = \sqrt{2}/2$, $d = \sqrt{5}/5$ and $\phi = \frac{2}{5}\pi$. The first three components of these vectors are in the normal space V_E , and the last three in the internal space V_I . The acceptance volume (the projection of the 6D unit cell onto V_I) corresponds to a triacontahedron.

In our numerical study, the cluster contain 11 965 sites. All sites are occupied by the same atoms with mass unity and the bond lengths are all taken to be equal to unity. By changing the force constants α and β we calculate the corresponding global densities of states and local densities of states for sites V_l ($l = 4, 5, 6, 7, 8, 9, 10, 12$), with l denoting its coordination number.

3. Spectrum analysis

Figure 1 shows the global density $\rho_G(\omega)$ of states. Figures 2(a)–2(h) show the local density of states for eight different kinds of site: V_{12} – V_4 , respectively. Comparing figure 1 with figure 2, we find that the different peaks exhibited in the global density of states are favoured by the special local configurations. Moreover, the larger the coordination number, the higher is the frequency of the mode that it favours. This result agrees with the observations of Liu and Tian [10] for an octagonal lattice.

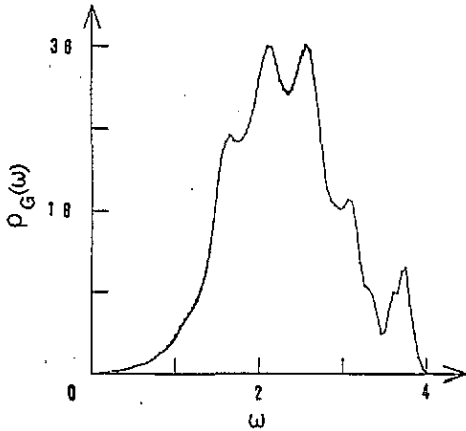


Figure 1. Global densities of states with constants $\alpha = \beta = 1$.

The character of the eigenstates is described by the spatial distribution of the vibrational amplitude.

(a) If all sites in the lattice vibrate with the same amplitude in the vicinity of their equilibrium position and for each site the vibrational displacement $u_l = u_0 \exp(i\omega t)$, then such an eigenstate is called the extended state.

(b) If the vibrational displacement $u = u(r) \exp(i\omega t)$, and the amplitude decays exponentially from the centre site $r = 0$, $u(r) \sim \exp(-r/\zeta)$ with localized length ζ , this vibrational state is localized, and with size ζ .

(c) If the above two conditions cannot be satisfied, the spatial distribution of amplitudes is in the character of a larger fluctuation having a maximum at a site and a series of subsidiary maxima at other sites which do not decay to zero; this eigenstate is called the 'critical' state or 'intermediate' state [2].

As we know, the local density of states is proportional to the square of the amplitude of the site [26, 27]; so we can obtain some information about the vibrational modes in the quasi-crystal from the calculation of the local density of states. Figure 3 shows the

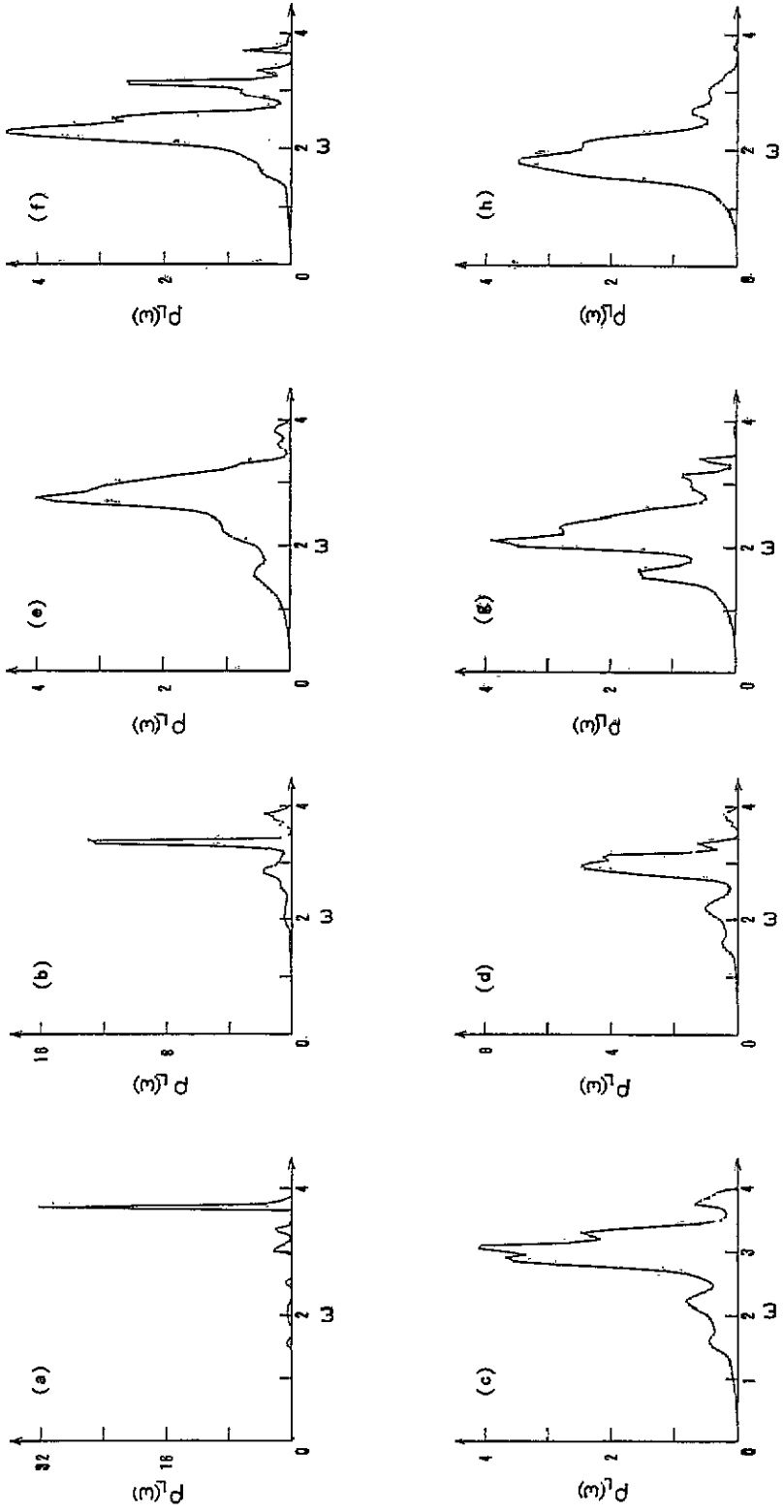


Figure 2. Local densities of states with constants $\alpha = \beta = 1$ for (a) V_{12} , (b) V_{10} , (c) V_6 , (d) V_8 , (e) V_7 , (f) V_6 , (g) V_5 and (h) V_4 sites.

local integrated density $\rho'_L(\omega)$ of states for eight kinds of site, namely V_{12} – V_4 . Analysis indicates that three kinds of typical eigenstate coexist in the 3D Penrose lattice. Extended states appear at low frequencies; all the other specific modes should be critical except the higher-frequency modes ω_{10} and ω_{12} , which are evidently localized. For example, the local density of states for site V_{12} (figure 3(a)) produces a sharp jump at ω_{12} . The mode has a much larger amplitude at this site and it significantly decreases at its nearest neighbours V_6 (figure 3(f)) and attenuates to zero at its second-nearest neighbours V_8 (figure 3(d)).

We can make an approximate calculation for ω_{12} under the isotropic model. When $\alpha = \beta$, equation (1) gives the isotropic potential

$$V = \frac{1}{2} \sum_{i,j}^{\text{NN}} \alpha |u_i - u_j|^2 \quad (4)$$

and the vector problem becomes a simple scalar problem; the vector notation for u can be dropped. With $|u_0\rangle$ representing the displacement of V_{12} , $|u_i\rangle$ ($i = 1, 2, \dots, 12$) the displacements of its 12 nearest neighbours and $|U_{ij}\rangle$ ($i = 1, \dots, 12; j = 1, \dots, 5$) the displacement of its second-nearest neighbours, we have

$$m \frac{\partial^2}{\partial t^2} |u_0\rangle = \sum_{i=1}^{12} \alpha (|u_0\rangle - |u_i\rangle). \quad (5)$$

Suppose that $|u_0\rangle = |u_a\rangle \exp(i\omega t)$; then

$$A |u_0\rangle = 12 |u_0\rangle - \sum_{i=1}^{12} |u_i\rangle \quad (6)$$

where $A = m\omega^2/\alpha$. For the 12 nearest neighbours, we obtain

$$A |u_i\rangle = 6 |u_i\rangle - |u_0\rangle - \sum_{j=1}^5 |U_{ij}\rangle. \quad (7)$$

Subtracting $6|u_i\rangle$ from both sides of equation (7), then we have

$$(A - 6) |u_i\rangle = -|u_0\rangle - \sum_{j=1}^5 |U_{ij}\rangle. \quad (8)$$

Substituting this into equation (7) and extracting the $|u_i\rangle$, we obtain a relation between $|u_0\rangle$ and $|U_{ij}\rangle$:

$$A(A - 6) |u_0\rangle = 12(A - 6) |u_0\rangle + 12 |u_0\rangle + \sum_{i,j} |U_{ij}\rangle. \quad (9)$$

As mode ω_0 is highly localized, $|U_{ij}\rangle$ is much smaller than $|u_0\rangle$; ignoring $|U_{ij}\rangle$, we have approximately

$$A(A - 6) = 12(A - 6) + 12. \quad (10)$$

The equation gives two roots; the reasonable root is $A = 13.58$, which gives $\omega = 3.69$ for $m = \alpha = 1$ in good agreement with our numerical result $\omega_{12} = 3.7$.

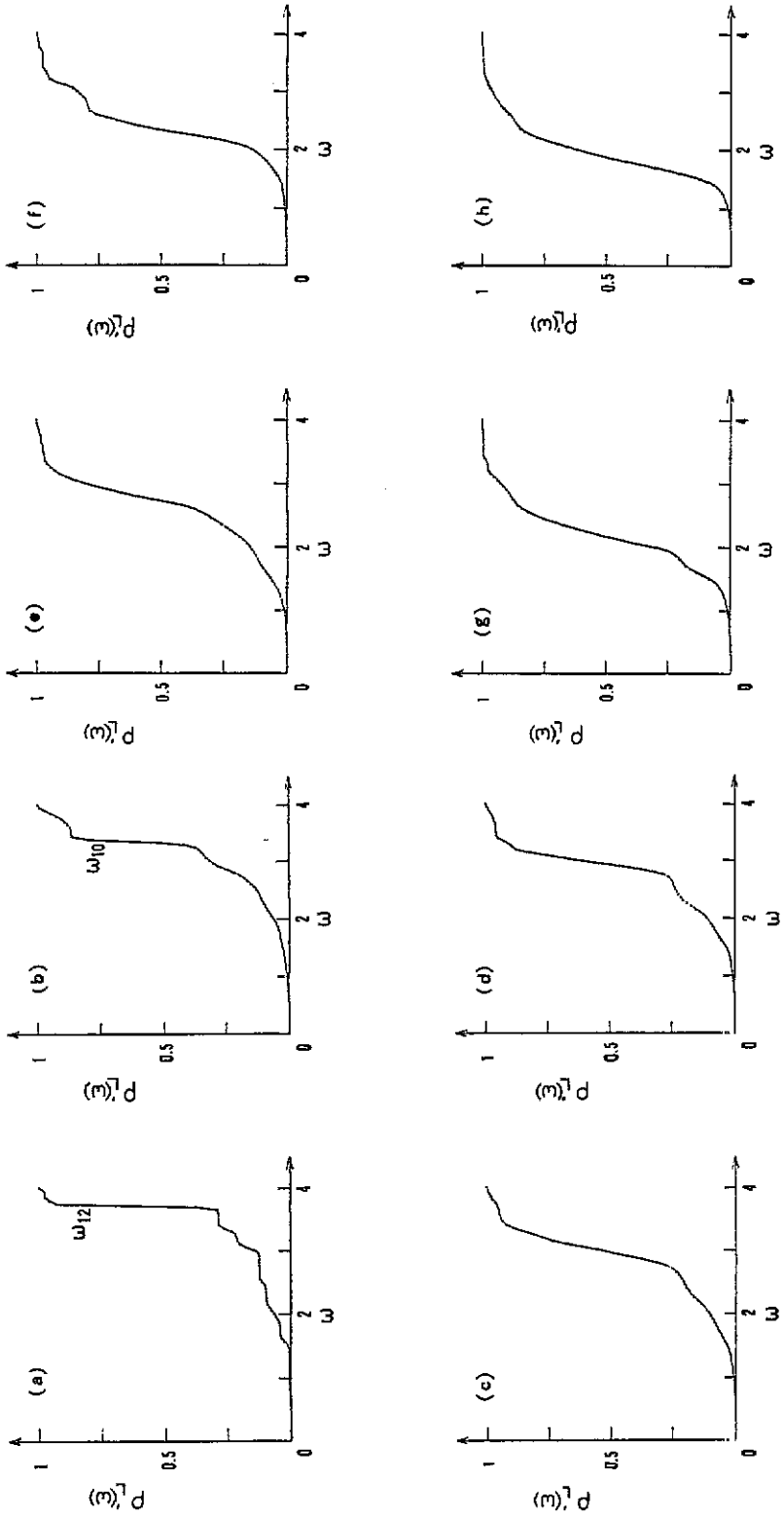


Figure 3. Local integrated densities of states with constants $\alpha = \beta = 1$ for (a) V_{12} , (b) V_{10} , (c) V_9 , (d) V_8 , (e) V_7 , (f) V_6 , (g) V_5 and (h) V_4 sites.

Figure 4 shows the global vibrational densities of states for the cluster with different force constant ratios, i.e. $\alpha/\beta = 1, 3, 10$ and 50 . To emphasize the low-frequency features, we adopt a logarithmic coordinate system; the horizontal axis is the logarithm of the angular frequency of vibration, and the vertical axis is the logarithm of the global vibrational densities of states. We observe the same crossover as that noticed by Liu and Tian [10, 11] in 2D quasi-crystals; in this figure, it is labelled ω_c . In a frequency regime both above and below ω_c the vibrational densities of states follow a power law $\rho_G(\omega) \propto \omega^2$. It is certain that below ω_c the vibrational densities of states are attributed to phonon excitations while above ω_c they are attributed to fracton-like excitations in terms of the conclusion of Liu and Tian [10, 11]. To check this, we amplify the low-frequency part of figure 2 in figure 5. Obviously, the densities remain the same, independent of sites below ω_c but vary with sites above ω_c . This suggests that, below ω_c , vibrational excitations are phonons with extended states while, above ω_c , they are fracton-like excitations with intermediate vibrational states [10, 11], following the scaling law $\rho_G(\omega) \propto \omega^{d_s-1}$ with $d_s = 3$. As discussed in the introduction, quasi-crystals can be regarded as fractals with a fractal dimension equal to the Euclidean dimension. Self-similarity covers the whole scale. When the wavelength is larger than the scale of the whole structure, i.e. the vibrational frequency is lower than the corresponding value ω_c , quasi-crystals are regarded as homogeneous and the vibrational elementary excitation is a phonon but, when the wavelength is smaller than the scale, i.e. the frequency is larger than ω_c , quasi-crystals appear to be a fractal structure, and the vibrational excitation is fracton like. So the crossover from phonon excitations to fracton-like excitations appears.

In addition, it can be observed from figure 4 that, when α/β is increasing, i.e. when the model gradually tends to the anisotropic model, the spectrum above ω_c gradually deviates from a power law. For the isotropic model, the interaction between atoms depends only on the magnitude of their relative displacements and has nothing to do with their direction. When a scale transformation is performed on the quasi-lattice, qualitatively the dynamic equation can be renormalized; thus the spectrum above ω_c follows a power law. However, for the anisotropic model, the dynamic equation cannot be renormalized, resulting in a deviation from the power law for the spectra above ω_c . This shows that, when $\omega > \omega_c$, $\rho_G(\omega) \propto \omega^{d_s-1}$ is relevant to the scale feature of the inner interaction in the quasi-lattice and is an intrinsic character of quasi-crystals. The fracton-like behaviour corresponding to this regime is different from phonons below ω_c which are only of homogeneous structure.

This statement is confirmed by the fractal dimension calculation d_f of the 3D Penrose lattice using a mass-volume scaling. The result is shown in figure 6, which gives $d_f \simeq 3$ as expected. For $d_s = 2d_f/d_w$ [12], we obtain the random-walk dimension $d_w = 2$. For $\langle r^2 \rangle \simeq t^{2/d_w} = t$, there will be no anomalous diffusion in this lattice.

The existence of another crossover frequency ω_s in the extremely low-frequency region is surprising. Below ω_s the scaling law yields $\rho_G(\omega) \propto \omega^{d-1}$ with $d = 2$, and the states are extended. As the spectral dimension is equal to Euclidean dimension, this type of state below ω_s should correspond to 2D surface phonons. The effect of free boundaries might unavoidably introduce some features near the spectra edge that are not genuine features of the bulk. As the diameter of a finite spherical cluster is apparently smaller than its circumference, the frequency ω_s is definitely located below ω_c .

We have presented the first investigation of vibrational excitations in a 3D Penrose lattice. Our calculations show the low-frequency part of the spectrum follows an ω^2 law which is in good agreement with recent investigations of vibrational properties in 3D quasi-crystals [12, 15, 16]. We give a detailed discussion of the low-frequency part, suggesting

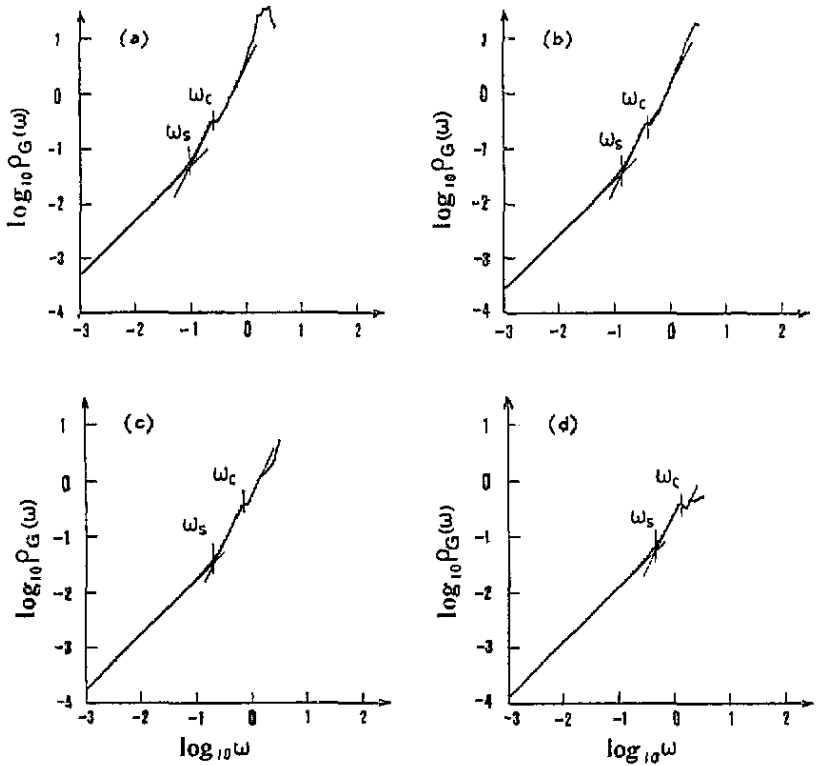


Figure 4. The vibrational densities of states for 3D Penrose tiling with the following constants: (a) $\alpha = \beta = 1$; (b) $\alpha = 3, \beta = 1$; (c) $\alpha = 10, \beta = 1$; (d) $\alpha = 50, \beta = 1$. The crossovers are indicated.

the existence of the crossover from phonon to fracton-like excitations; probably the pseudo-gap obtained by Los and Janssen is this crossover that we observed. The well defined propagating excitations (phonons) observed by Hafner and Krajci in their investigation of the excitations in rational approximants to quasi-crystals [15] are the extended phonons that we found below ω_c , and high-frequency localized modes [16] are also obtained in our calculation.

4. Conclusions

The vibrational densities of states for a 3D Penrose tiling with various force constants are calculated numerically. It is found that there exist two crossover frequencies ω_s and ω_c . The first can be attributed to crossover from surface phonon excitations to bulk phonon excitations and the second is explained as a crossover from phonon excitations to fracton-like excitations. The phonons follow the scaling law ω^{d-1} , where d is the Euclidean dimension equal to 3 and 2 for the bulk and the surface phonons, respectively. The spectral features in the fracton-like excitation frequency regime depend on the force constants α and β ; when $\alpha/\beta = 1$ or α/β is not very large, the spectrum satisfies a scaling law $\rho_G(\omega) \propto \omega^{d_s-1}$ with $d_s = 3$ in the present particular case. Compared with phonon excitations, fracton-like excitations are non-extended. In the high-frequency regime, some specific vibrational modes are exhibited; they favour different kinds of local configuration.

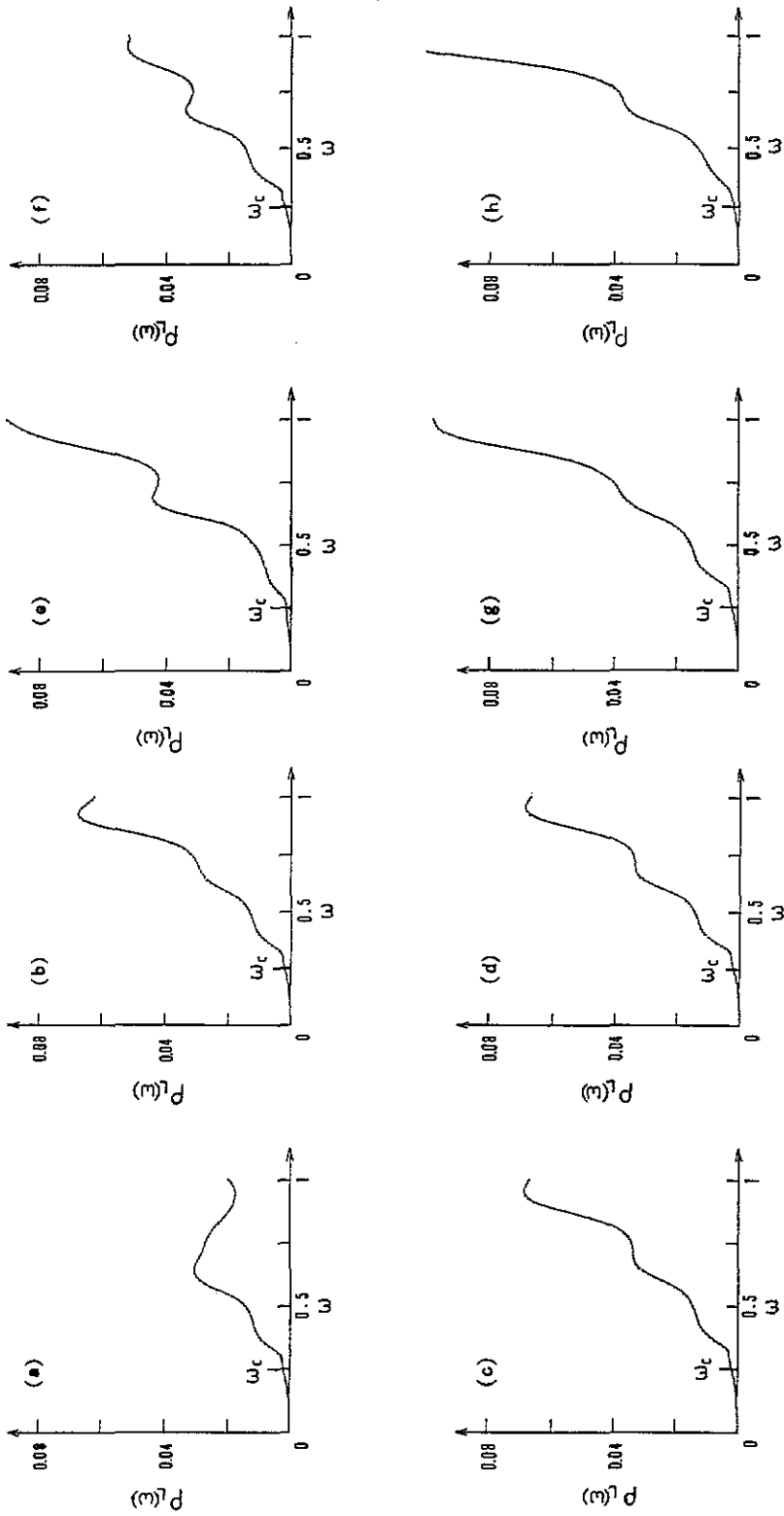


Figure 5. Local densities of states (α) for V_{12} , (b) for V_{10} , (c) for V_9 , (d) for V_8 , (e) for V_7 , (f) for V_6 , (g) for V_5 and (h) for V_4 , with $\alpha = \beta = 1$. It is a simple magnification of figure 2 in the low-frequency part.

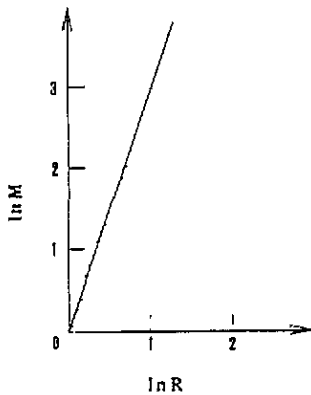


Figure 6. Log-log plot of the mass-radius diagram. This shows that the fractal dimension of the 3D Penrose tiling is 3.

Acknowledgments

Support from the National Natural Science Foundation of China and Foundation for a PhD Graduate of the National Committee of Education is acknowledged.

References

- [1] Schechtman D S, Blech I, Gratias D and Cahn J W 1984 *Phys. Rev. Lett.* **53** 1951
- [2] Kohmoto M and Banavar J R 1986 *Phys. Rev. B* **34** 563
- [3] Lohmoto M, Kadanoff L P and Tang C 1983 *Phys. Rev. Lett.* **50** 1870
- [4] Ostlund S, Pandit R, Rand D, Schellnhuber H J and Siggia E D 1983 *Phys. Rev. Lett.* **50** 1873
- [5] Nori F and Rodrigues J P 1986 *Phys. Rev. B* **34** 2207
- [6] Niu Q and Nori F 1986 *Phys. Rev. Lett.* **57** 2057
- [7] Fujiwara T, Kohmoto M and Tokihiro T 1989 *Phys. Rev. B* **40** 7413
- [8] Choy T C 1985 *Phys. Rev. Lett.* **55** 2915
- [9] Odagaki Y and Nguyen D 1986 *Phys. Rev. B* **33** 2184
- [10] Liu Z and Tian Decheng 1992 *J. Phys.: Condens. Matter* **4** 6343
- [11] Liu Z and Tian Decheng 1992 *Phys. Lett.* **168A** 429-32
- [12] Los J and Janssen T 1990 *J. Phys.: Condens. Matter* **2** 9553
- [13] Los J, Janssen T and Gahler F 1993 *J. Physique* **1** 3 107
- [14] Los J, Janssen T and Gahler F 1993 *J. Non-Cryst. Solids* **153-4** 581
- [15] Hafner J and Krajci M 1993 *Europhys. Lett.* **21** 31
- [16] Hafner J and Krajci M 1993 *Phys. Rev. B* **47** 1084
- [17] Elser V 1985 *Phys. Rev. B* **32** 4892
- [18] Rokhsa D S, Mermin N D and Wright D C 1988 *Phys. Rev. B* **37** 8145
- [19] Alexander S and Orbach R 1983 *J. Physique Lett.* **43** L625
Rammal R and Toulouse G 1983 *J. Physique Lett.* **44** L13
- [20] Feng S 1985 *Phys. Rev. B* **32** 5793
- [21] Feder J 1988 *Fractals* (New York: Plenum)
- [22] Yakubo K and Nakayama T 1989 *Phys. Rev. B* **40** 517
- [23] Peng G and Tian D 1991 *J. Phys.: Condens. Matter* **3** 1065
- [24] Peng G and Tian D 1991 *Phys. Rev. B* **43** 8572
- [25] Haydock R, Heine V and Kelly M 1972 *J. Phys. C: Solid State Phys.* **5** 2845
- [26] Haydock R, Heine V and Kelly M 1975 *J. Phys. C: Solid State Phys.* **8** 2591
- [27] Nex C M M 1986 (Cambridge: Cambridge Fortran Library)
- [28] Zia R K P and Dallas W J 1985 *J. Phys. A: Math. Gen.* **18** L341
- [29] Elser V and Henley C L 1985 *Phys. Rev. Lett.* **55** 2883
- [30] Janssen T 1986 *Acta Crystallogr. A* **42** 261
- [31] Bak P 1986 *Phys. Rev. Lett.* **56** 861
- [32] Socolar J E S, Steinhardt P J and Levine D 1985 *Phys. Rev. B* **32** 5547